Kinetics of the Termolecular Insertion Reaction of Ground State Rhodium with Methane

Mark L. Campbell

Chemistry Department
United States Naval Academy
Annapolis, Maryland 21402

Received March 13, 1997

There has been considerable interest in transition metal (TM)/hydrocarbon chemistry due to attempts to understand the activation of carbon−hydrogen bonds in catalytic processes.[1] Extensive experimental and theoretical work has focused on gas phase TM reactions with CH_4.[2−4] The activation of the C−H bond in methane is a unique challenge among the hydrocarbons due to its unusual strength (i.e., the C−H bond energy in methane (438 kJ/mol) is 18 kJ/mol greater than the C−H bond energy in ethane).[2d] Of the TM atoms studied thus far, only Pt has been found to react with CH_4 in the gas phase.[3] Organometallic compounds of Rh are the only compounds of second row TMs found to be active in homogeneous oxidative addition to alkanes,[5] while calculations predict gas phase Rh reacts with CH_4 by an insertion mechanism without a barrier.[4] However, Rh does not react at a measurable rate with CH_4 in a fast flow tube at total pressures of up to 1.5 Torr,[4] while no reaction was observed for Rh clusters in CH_4.[6] In this paper, we report the gas phase chemical removal of the $a^4F_{9/2}$ ground state of Rh in the presence of CH_4 by a termolecular insertion mechanism.

Pseudo-first-order kinetic experiments ([Rh] ≪ [CH_4]) were performed in an apparatus with slowly flowing gas using a laser photolysis/laser-induced fluorescence (LIF) technique. The experimental apparatus and technique have been described in detail elsewhere.[7]

Rh atoms were detected via LIF following the 248 nm photodissociation of (acetylacetanato)dicarbonylrhodium [Rh(acac)$(CO)_2$] using an excimer laser. Reactions were monitored by observing the temporal decay of Rh atoms as a function of CH_4 partial pressure. Temporal profiles were collected by measuring the LIF signal at different probe laser delays relative to the photolysis laser. The laser delays were varied by a digital delay generator.

CH_4 (MG Industries, 99.999%), Ar (Potomac Airgas, Inc., 99.998%), and Rh(acac)$(CO)_2$ (Strem, 99.9%) were used as received.

Rh atoms in all of the states with less than 13 000 cm^{-1} of electronic energy were observed under these experimental conditions. Careful measurements of the relative populations of these states were not determined; however, we estimate approximately 50% of the Rh atoms are produced in excited states based on the growth in the temporal profile of the ground state in the absence of CH_4.

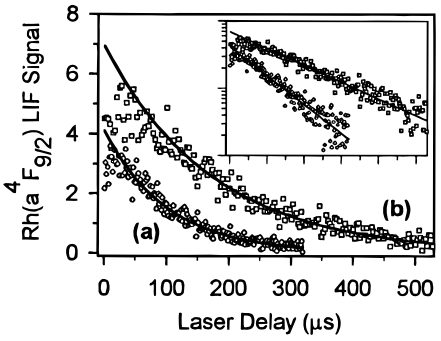

Figure 1. Typical Rh($a^4F_{9/2}$) temporal profiles; T = 296 K, P_{total} = 100.0 Torr. (a) $P(CH_4)$ = 0.77 Torr, τ = 98 μs. (b) $P(CH_4)$ = 0.40 Torr, τ = 173 μs. The inset is a logarithm plot of the data.

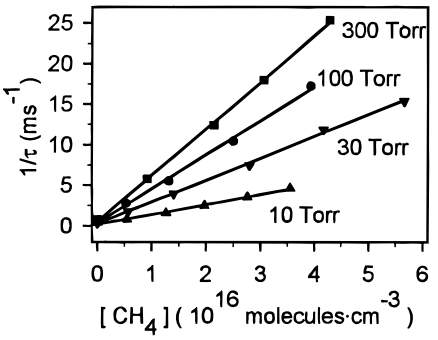

Figure 2. Typical plots for determining k_{obsd} for Rh($a^4F_{9/2}$) + CH_4 in Ar buffer indicating the dependence of the observed rate constant on total pressure. The solid line for each set of data is a linear regression fit from which k_{obsd} is obtained.

The decay rates of the ground state ($a^4F_{9/2}$) of Rh as a function of CH_4 partial pressure in Ar buffer were investigated at different total pressures at room temperature (297 ± 1 K). A majority of the decay profiles showed growth (i.e., nonexponential behavior) at the beginning of the decays, as shown in Figure 1. This behavior is attributed to the relaxation of the higher electronic states to the ground state. In the presence of CH_4, the electronically excited states react/relax much more rapidly than the ground state. Thus, slight growth at short laser delays is typically observed for the ground state in the presence of CH_4, and exponential decays are observed at longer laser delays. Once the electronically excited states have relaxed, the loss of ground state Rh is described by the first-order decay constant, k_1,

$$k_1 = 1/\tau = k_d + k_{obsd}[CH_4] \quad (1)$$

where τ is the first-order time constant for the removal of Rh under the given experimental conditions, k_d is the loss term due to diffusion out of the detection zone and reaction with the precursor, and k_{obsd} is the second-order rate constant. Time constants were determined by adjusting the range of the linear regression analysis (i.e., the range did not include the beginning of the decay when growth was present). Typical decays were analyzed after a delay of approximately one reaction lifetime and included data for a length of two to three reaction lifetimes. The observed second-order rate constant is determined from the slope of a plot of $1/\tau$ vs [CH_4]. Typical plots for obtaining the second-order rate constants are presented in Figure 2. The relative uncertainty (i.e., reproducibility) of the rate constants is estimated at ±10%. The absolute uncertainties are estimated

(1) (a) Ritter, D.; Weisshaar, J. C. *J. Am. Chem. Soc.* **1990**, *112*, 6425. (b) Ritter, D.; Carroll, J. J.; Weisshaar, J. C. *J. Phys. Chem.* **1992**, *96*, 10636. (c) Carroll, J. J.; Haug, K. L.; Weisshaar, J. C. *J. Am. Chem. Soc.* **1993**, *115*, 6962. (d) Weisshaar, J. C. In *Gas-Phase Metal Reactions*; Fontijn, A., Ed.; Elsevier: Amsterdam, 1992.

(2) (a) Blomberg, M. R. A.; Siegbahn, P. E. M.; Nagashima, U. *J. Am. Chem. Soc.* **1991**, *113*, 424. (b) Carroll, J. J.; Weisshaar, J. C. *J. Am. Chem. Soc.* **1993**, *115*, 800. (c) Parnis, J. M.; Lafleur, R. D.; Rayner, D. M. *J. Phys. Chem.* **1995**, *99*, 673. (d) Senba, K.; Matsui, R.; Honma, K. *J. Phys. Chem.* **1995**, *99*, 13992. (e) Honma, K. *J. Chin. Chem. Soc.* **1995**, *42*, 371.

(3) (a) Carroll, J. J.; Weisshaar, J. C.; Siegbahn, P. E. M.; Wittborn, C. A. M.; Blomberg, M. R. A. *J. Phys. Chem.* **1995**, *99*, 14388. (b) Carroll, J. J.; Weisshaar, J. C. *J. Phys. Chem.* **1996**, *100*, 12355.

(4) (a) Blomberg, M. R. A.; Siegbahn, P. E. M.; Svensson, M. *J. Am. Chem. Soc.* **1992**, *114*, 6095. (b) Carroll, J. J.; Haug, K. L.; Weisshaar, J. C.; Blomberg, M. R. A.; Siegbahn, P. E. M.; Svensson, M. *J. Phys. Chem.* **1995**, *99*, 13955.

(5) (a) Jones, W. D.; Feher, F. J. *J. Am. Chem. Soc.* **1982**, *104*, 4240. (b) Periana, R. A.; Bergman, R. G. *J. Am. Chem. Soc.* **1986**, *108*, 7332. (c) Weiller, B. H.; Wasserman, E. P.; Bergman, R. G.; Moore, C. B.; Pimentel, G. C. *J. Am. Chem. Soc.* **1989**, *111*, 8288.

(6) Zakin, M. R.; Cox, D. M. *J. Chem. Phys.* **1988**, *89*, 1201.

(7) Campbell, M. L.; McClean, R. E. *J. Chem. Soc., Faraday Trans.* **1995**, *91*, 3787.

S0002-7863(97)00816-0 CCC: $14.00

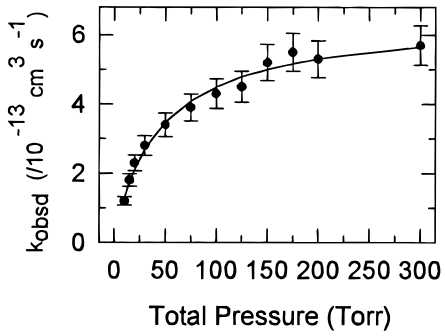

Figure 3. Plot of observed second-order rate constant for the reaction of Rh($a^4F_{9/2}$) with CH_4 against pressure of Ar buffer gas at room temperature. Error bars represent ±10%. The solid line is a fit to eq 2.

at ±30% and are based on the sum of the statistical scatter in the data, uncertainty in the flow meter, flow controller, and pressure readings, and errors associated with incomplete mixing.

The observed room temperature rate constants are dependent on total pressure indicating a termolecular process. The variation with total pressure is illustrated in Figure 3. The solid line through the data in Figure 3 is a fit to the simplified falloff expression of Troe[8]

$$\log k = \log\frac{(k_o[M])}{1 + (k_o[M])/k_\infty} + \frac{\log F_c}{1 + [\log(k_o[M]/k_\infty)]^2} \quad (2)$$

where k_o and k_∞ are the limiting low-pressure third-order and high-pressure second-order rate constants, respectively, [M] is the buffer gas number density, and F_c is the broadening factor.

The values for k_o, k_∞, and F_c in argon buffer at room temperature are $(5.3 \pm 0.9) \times 10^{-31}$ cm^6 s^{-1}, $(6.7 \pm 0.7) \times 10^{-13}$ cm^3 s^{-1}, and 0.93 ± 0.14, respectively. Uncertainties are $\pm\sigma$. The previous observation of no reaction ($k < 3 \times 10^{-14}$ cm^3 s^{-1}) between Rh and CH_4 at pressures of only 0.8 Torr is consistent with the rate constants and termolecular parameters reported here.[4b]

The primary focus of this study was on the $a^4F_{9/2}$ state; however, the excited states were also studied to determine the effect on the ground state temporal decay profiles due to physical quenching. Table 1 lists the measured removal rate constants at 20 Torr total pressure. The smallest rate constant measured (1.8×10^{-12} cm^3 s^{-1}) for the excited states was for the $a^4P_{5/2}$ and $a^2P_{3/2}$ states. This rate constant is over three times larger than the largest measured rate constant for the ground state. Thus, excited states do not interfere with the temporal decays of the ground state beyond one reaction lifetime.

Blomberg and co-workers have performed calculations for the reactions of all of the gas phase second row TMs with CH_4.[4]

(8) Troe, J. *J. Phys. Chem.* **1979**, *83*, 114.
(9) Moore, C. E. *NBS Circular 467*; U.S. Department of Commerce: Washington, DC, 1971; Vol. III.
(10) Duquette, D. W.; Lawler, J. E. *J. Opt. Soc. Am. B* **1985**, *2*, 1948.

Table 1. Second-Order Removal Rate Constants for the Low-Lying States of Rhodium in CH_4 (P_{total} = 20.0 Torr, Ar buffer)

electronic state	electronic[a] energy (cm^{-1})	transition[b] wavelength (nm)	k_{obsd} ($/10^{-13}$ cm^3 s^{-1})
d^8s^1 $a^4F_{9/2}$	0	369.24	2.3[c]
d^8s^1 $a^4F_{7/2}$	1530	370.09	*d*
d^8s^1 $a^4F_{5/2}$	2598	380.68	*e*
d^9 $a^2D_{5/2}$	3310	369.07	1300
d^8s^1 $a^4F_{3/2}$	3473	371.30	43
d^9 $a^2D_{3/2}$	5658	378.85	2200
d^8s^1 $a^2F_{7/2}$	5691	379.32	1800
d^8s^1 $a^2F_{5/2}$	7791	408.28	24
d^8s^1 $a^4P_{5/2}$	9221	382.85	18
d^8s^1 $a^4P_{3/2}$	10313	399.56	59
d^8s^1 $a^4P_{1/2}$	11006	405.34	36
d^8s^1 $a^2P_{3/2}$	11968	497.99	18
d^7s^2 $b^4F_{9/2}$	12723	598.36	23

[a] Reference 9. [b] Reference 10. [c] The measured rate constants are 1.2, 1.8, 2.8, 3.4, 3.9, 4.3, 4.5, 5.2, 5.5, 5.3, and 5.7×10^{-13} cm^3 s^{-1} for 10, 15, 30, 50, 75, 100, 125, 150, 175, 200, and 300 Torr, respectively. [d] Exhibited biexponential behavior in the presence of methane; the rate constant, however, is large, based on a reaction time constant of only 1.1 μs in 0.37 Torr CH_4. [e] Although observed, the LIF signal for this state was too weak to measure rate constant values.

The barriers to CH activation for the TMs to the left of the second row series are higher than the barriers to the right, with a minimum at Rh. The mechanism predicted for Rh reacting with CH_4 based on these calculations is the termolecular associative insertion channel:

$$Rh + CH_4 + M \rightarrow H{-}Rh{-}CH_3 + M \quad (3)$$

For Rh, no potential barrier to CH insertion is encountered on the low-spin (doublet) surface with the calculated energy at the transition state geometry lying 5.9 kJ/mol below the reactants, while the potential well for $H{-}Rh{-}CH_3$ is 80 kJ/mol lower than that of the reactants.[4] The unusual reactivity of Rh with CH_4 is attributed to its uniquely balanced pattern of low-lying atomic states. Calculations indicate atomic states with the lowest repulsion toward CH_4 are d^n states and the strongest bonds are formed to d^{n-1} s^1 states, where n is the number of valence electrons. Thus, the reactivity of Rh is attributed to its ground state having a high-spin $4d^85s^1$configuration which readily forms the sd hybrid orbitals necessary to make two σ bonds.

Furthermore, its $4d^9$ configuration lies at low energy allowing the atom to minimize repulsion at long range. The rate constants of the d^9 states observed here experimentally (Table 1) verify the small repulsion associated with these states.

Acknowledgment is made to the Donors of the Petroleum Research Fund, administered by the American Chemical Society, for partial support of this research. This research was supported by a Cottrell College Science Award of Research Corporation. M.L.C. is a Henry Dreyfus Teacher-Scholar.

JA9708169